https://doi.org/10.5194/egusphere-2026-403
Preprint. Discussion started: 10 February 2026

A prototype algorithm for daily water hyacinth monitoring at Hartbeespoortdam, South Africa, from Sentinel-3 OLCI data

Marloes Penning de Vries[1], Cletah Shoko[2], Timothy Dube[3], Kgabo Humphrey Thamaga[4], Suhyb Salama[1]

[1]Faculty of Geo-Information Science and Earth Observation (ITC), University of Twente, Enschede, Netherlands
[2]School of Geography, Archaeology and Enviromental Studies, University of Witwatersrand, Pretoria, South Africa
[3]Department of Earth Science, University of the Western Cape, Belville, South Africa
[4]Faculty of Science and Agriculture, University of Fort Hare, Fort Hare, South Africa

Correspondence to: Marloes Penning de Vries (m.j.m.penningdevries@utwente.nl)

Abstract. Water HYacinth (WHY) is one of the world's most disturbing invasive aquatic plant species, characterised by a high spatial and temporal variability. Remote sensing is a valuable approach to monitor WHY, as the dense, floating mats of vegetation can be detected using various satellite instruments, for example, OLCI on Sentinel-3. The multi-spectral instrument features only moderate spatial resolution (300 m), however, it achieves global coverage in two days, and with two instruments currently in orbit, it provides an opportunity to monitor WHY at near-daily resolution. This is crucial, considering that WHY cover patterns are highly variable due to the plants' rapid reproduction and the influences of wind and hydrodynamics. We present the development of an algorithm for the creation of daily WHY maps by: (1) deriving WHY cover patterns from both OLCI instruments using the Normalized Difference Vegetation Index, NDVI; (2) merging the data sets into one with near-daily resolution; and (3) filling the gaps (due to missing observations or cloud interference) using a spatial-temporal interpolation scheme. We show that the gap-filling strategy leads to a consistent daily time series of WHY cover for the study region and increases the number of days with observations by 55%. A leave-one-out analysis showed that the interpolation algorithm performs well even for longer periods without observations, unless WHY cover patterns change abruptly. The presented algorithm is computationally light-weight and, although developed for Hartbeespoortdam Reservoir (South Africa), is easily adaptable for use with other water bodies. The prototype WHYmapping algorithm was used to analyse eighteen months of data (July 2022 – December 2023). In the future, long time series of daily WHY maps may provide an evaluation tool for WHY management and benefit water management strategies directly by allowing continuous monitoring of WHY.

1 Introduction

Ecosystems around the world are being disturbed by the effects of human presence. Lake ecosystems are particularly affected by land use changes, pollution, and the introduction of alien species (Jenny et al., 2020). The water hyacinth

https://doi.org/10.5194/egusphere-2026-403
Preprint. Discussion started: 10 February 2026

(*Eichhornia crassipes*) is an invasive species in many freshwater lakes and rivers around the planet. Its rapid proliferation is a symptom of excess nutrient inflow from agricultural fields, industry, inadequately treated wastewater and other sources (Coetzee et al., 2017).

Water Hyacinth (WHY) are free-floating plants that form patches that can be so dense that boat traffic cannot pass. WHY clog water treatment plants and inlets of hydroelectric dams, block access to drinking water for humans, cattle and wildlife (Kleinschroth et al., 2021). Lakes and reservoirs covered by WHY are rendered unattractive to tourists. Moreover, the weed blocks sunlight from reaching the lower levels, affecting aquatic life (Coetzee et al., 2017).

There have been different approaches to manage WHY infestations, such as: mechanical removal, herbicide spraying, and the introduction of weevils and other insects feeding on the plant (Coetzee et al., 2017; Fusilli et al., 2013; Güereña et al., 2015; Kleinschroth et al., 2021). The high water content of the plants makes mechanical removal highly labour intensive, and because it is unfeasible to eradicate the weed, the procedure needs to be repeated on a regular basis. Herbicides specifically targeted at WHY are effective and comparatively cheap in application, but the sinking and subsequent decaying of dead plant material may cause anoxia at the bottom of the water body. Weevils have been shown to be effective at increasing WHY mortality and promising results have been achieved at Hartbeespoort dam in South Africa (Jones et al., 2018), but the insects fail to decrease plant cover appreciably (Harun et al., 2021). A systematic investigation of WHY responses to various management practices has been missing in the literature to date. Such a systematic investigation requires regular monitoring of WHY cover over a period of time that is sufficiently long to distinguish effects of applied measures from natural variability and other factors affecting the spread and movement of the plants.

WHY is a rapidly spreading aquatic plant, which reproduces via vegetative reproduction, but also produces seeds that can survive several years without water (Albano Pérez et al., 2011). Its growth rate depends mainly on temperature and nutrient level of the water (Wilson et al., 2005) and, correspondingly, time series of WHY occurrence have been found to feature a distinct seasonal dependence on temperature and/or precipitation (Dersseh et al., 2020; Janssens et al., 2022; Kleinschroth et al., 2021). The high degree of interannual variation observed in different regions was mainly attributed to variability in rainfall (Fusilli et al., 2013; Gbetkom et al., 2023; Janssens et al., 2022), lake water level (Dersseh et al., 2020; Worqlul et al., 2020), changing control measures and urban land cover (Kleinschroth et al., 2021). Because WHY is a free-floating plant, its dynamics are governed by winds and currents (Coetzee et al., 2017), hence, the distribution of the plants on a water body varies from day to day. To monitor WHY for the purpose of understanding drivers of WHY proliferation, of evaluating control measures or issue early warnings, observations at daily resolution – or better – are required. However, the high variability of the species and the relative inaccessibility of affected sites complicate the acquisition of data suitable for long-term time series analysis.

Satellite-borne sensors are ideally suited to produce data sets with which aquatic plants can be systematically monitored. Floating plants, like WHY, form dense mats that are clearly visible from space, and satellite sensors record regular, consistent observations over large parts of the globe. Floating vegetation can be clearly distinguished from open water or

https://doi.org/10.5194/egusphere-2026-403
Preprint. Discussion started: 10 February 2026

submerged vegetation by making use of radiation detected in the visible to near-infrared bands of instruments like the Multi-
65 Spectral Imager (MSI) and the Ocean and Land-Colour Imager (OLCI) on ESA's platforms Sentinel-2 and -3, respectively (Donlon et al., 2012; Drusch et al., 2012). In addition to the sensors on the Sentinel missions, a number of satellite sensors proved useful for the observation of WHY in the past. These include the MODerate resolution Imaging Spectroradiometer (MODIS), MEdium Resolution Imaging Spectrometer (MERIS), and various evolutions of the Enhanced Thematic Mapper (ETM) on Landsat platforms, to name a few. A recent overview is provided by (Datta et al., 2021).

70 Identification of plants' location and extent from satellite is based on spectral reflectances (Bayable et al., 2023; Cavalli et al., 2009) and/or spectral indices (Cheruiyot et al., 2014; Fusilli et al., 2013; Kleinschroth et al., 2021). These studies implicitly or explicitly make use of the spectral signature of green, leafy vegetation, which differs markedly from that of many other surfaces, including clear water, in the visible wavelength range (e.g. (Cavalli et al., 2009)). The difference in surface roughness between water and floating vegetation can also be exploited for WHY detection using satellite-borne radar, as
75 shown for the Synthetic Aperture Radar-C on Sentinel-1 (Simpson et al., 2022). In many cases, machine-learning techniques were employed to account for non-linear and unexpected relationships between variables (Bayable et al., 2023; Lin et al., 2021; Piaser and Villa, 2023; Thamaga and Dube, 2018).

Previous studies on WHY used data from instruments with relatively high spatial resolution, but low overpass frequency, such as Landsat or Sentinel-2 (overpasses every 5-10 days). In cases where instruments with daily overpasses were used,
80 e.g., MODIS in (Kleinschroth et al., 2021), the data were averaged on a monthly time scale. Considering the high spatial and temporal variability of the species, the time resolution of these studies is not sufficient to track the rapid movements of WHY. This emphasizes the need for the development of an algorithm to provide better temporal sampling of floating vegetation.

We present the development of a straightforward, computationally light-weight algorithm to derive daily maps of WHY
85 cover of inland water bodies. The algorithm uses OLCI data to detect floating aquatic plants and applies a sophisticated gap-filling method to yield daily, gap-free maps of WHY cover. The method was developed for Hartbeespoortdam reservoir, South Africa, but can easily be adapted to other water bodies of sufficient size.

2. Data and methods

2.1 Study area description

90 The study was conducted in the Hartbeespoortdam reservoir (25° 43′ 32″ S, 27° 50′ 54″ E) which is located in the North West Province of South Africa (Fig. 1). The reservoir, in the following called "Dam", is fed by the Crocodile and Jukskei rivers, covers an area of 19 km^2 and features a maximum depth of 45 m. The Dam plays an important role by providing water for irrigation and to surrounding communities. In addition, the Dam is a major tourist attraction area, supporting various recreational facilities, fishing and boat cruising. It is, therefore, a significant natural resource for economic

https://doi.org/10.5194/egusphere-2026-403
Preprint. Discussion started: 10 February 2026

95 development and supporting human livelihood. However, since the 1970s the Dam suffers strongly from the invasion of floating plants, particularly WHY. Proliferation of the nutrient-loving invasive species is enabled by the influx of wastewater and the consequent eutrophication of the reservoir. Numerous efforts have been made to remove WHY by mechanical, chemical or biological means at considerable costs (e.g., (Kleinschroth et al., 2021)), but these have not led to eradication of the species. In highly eutrophic waters, the high proliferation rate coupled with long-term viability of WHY seeds makes
100 eradication nearly impossible; hence WHY are expected to remain present as long as lake nutrient levels remain high (Coetzee and Hill, 2012).

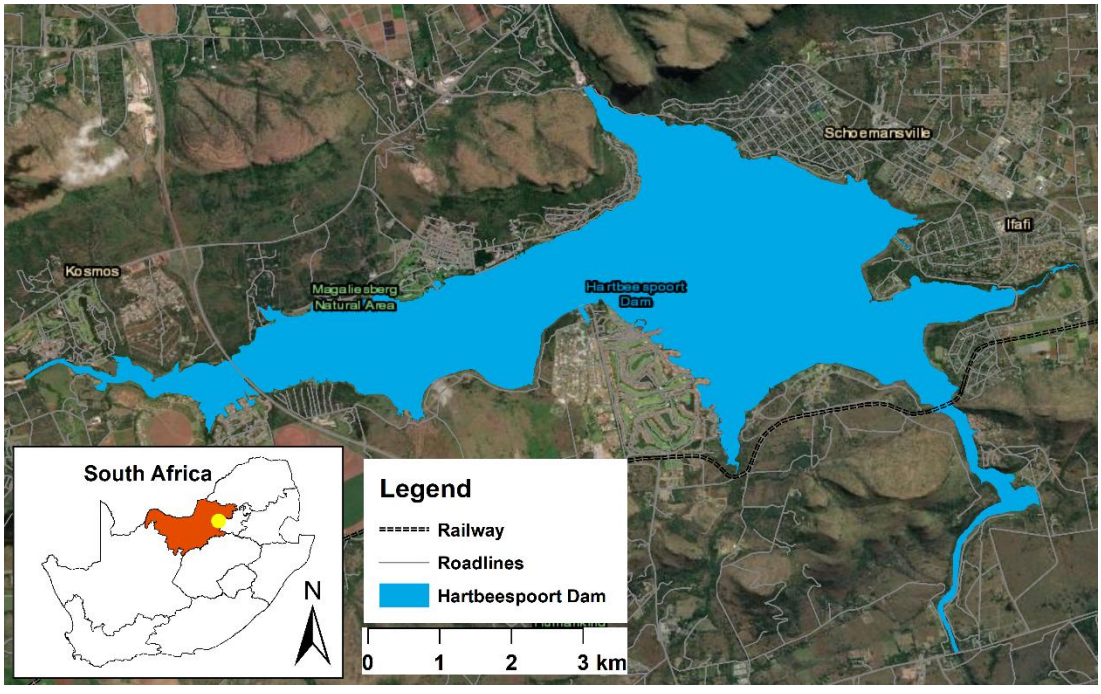

Figure 1: Location of the study area, Hartbeespoortdam reservoir in South Africa (figure made using ArcGIS software).

2.2. Satellite data

105 Data used within the study are from the OLCI sensors on Sentinel-3 satellites A and B; the details of the data set are presented in Table 1. OLCI was specifically designed for ocean-monitoring purposes, but is also very suitable for monitoring of vegetation over land – albeit at a lower spatial resolution than dedicated land surface imagers, such as MSI on Sentinel-2 (Drusch et al., 2012). With two instruments in operation, OLCI observes locations near the equator with a near-daily frequency.

110 OLCI level-1C data were obtained from the Copernicus Data and Information Access Service (WeKEO, www.wekeo.eu).

Table 1. Characteristics of OLCI on ESA missions Sentinel-3 (Donlon et al., 2012).

https://doi.org/10.5194/egusphere-2026-403
Preprint. Discussion started: 10 February 2026

Platform	**Sentinel-3**
Instrument	Ocean and Land Colour Imager (OLCI)
Start of operations	2016 (3A) and 2018 (3B)
Overpass time (local daytime)	10:00 AM
Overpass frequency (equator)	Every 1.1 days
Spatial resolution (IFOV at sub-satellite point)	300 m
Bands	21 channels in VIS/NIR
Level	1-C (Top of Atmosphere , ToA)
Observation range	01-07-2022 to 31-12-2023
Total number of images	OLCI-S3A: 303 OLCI-S3B: 280

2.3. WHYmapping algorithm

Daily maps of WHY coverage were derived from OLCI Level-1C radiances, which were analyzed using python scripts written for the purpose. This section describes the algorithm used to derive daily WHY maps.

The identification of WHY in OLCI data relies on the Normalized Difference Vegetation Index, NDVI. The NDVI was introduced to identify leafy green terrestrial vegetation half a century ago (Tucker, 1979), but it has only recently been applied to the detection of aquatic vegetation. The distinct red-edge information included in NDVI makes it highly suitable for distinguishing WHY from algal blooms (Cheruiyot et al., 2014; Dersseh et al., 2020; Fusilli et al., 2013; Gbetkom et al., 2023; Kleinschroth et al., 2021), although the signal may be contaminated by signals from green algae or very still waters.

Other, vegetation indices have been suggested (e.g., (Villa et al., 2014)), yet here we make use of the NDVI due to its applicability to a large number of sensors, its widespread use and its well-characterized behaviour (Huang et al., 2021). The NDVI is calculated from OLCI L1C top-of-atmosphere (TOA) radiances according to the following equation:

$$N_V = \frac{R_{\lambda 1} - R_{\lambda 2}}{R_{\lambda 1} + R_{\lambda 2}} \quad (1)$$

With $R_{\lambda 1}$ and $R_{\lambda 2}$ the radiance at the wavelength bands λ1 and λ2 in the near-infrared and red spectral ranges, respectively. Here, the NDVI is calculated from broad-band radiances in the near-infrared (bands 16-18 centered at 779, 865, and 885 nm) for λ1 and in the red range for λ2 (bands 7-10 centered at 620, 665, 674, and 681 nm), following the settings used for OLCI in the Copernicus Global Land Operations NDVI product (Swinnen and Toté, 2022).

From an inspection of MSI and OLCI RGB images it was found that WHY can be detected through a thin layer of clouds. Hence, it is not desirable to use a strict cloud filter, as this could remove a considerable amount of useful WHY observations.

https://doi.org/10.5194/egusphere-2026-403
Preprint. Discussion started: 10 February 2026

Observations strongly affected by clouds, which could produce false negatives, were removed using a threshold based on the ratio of reflectances in the blue (band 2) and green (band 4) spectral region. A "band ratio blue-green (BR_{BG})" is defined for this purpose:

$$BR_{BG} = \frac{R_{blue}}{R_{green}} \quad (2)$$

Clouds reflect radiation in the blue and green range equally, hence the presence of clouds in a scene causes BR_{BG} values to approach 1, which is the limiting case of scene completely covered by an optically thick, perfectly white cloud. Empirically it was found that a threshold value of BR_{BG} = 1.2 was suitable to remove scenes where clouds dominated the observed radiance to such an extent that WHY could not be identified. Hence, scenes where BR_{BG} does not exceed 1.2 were considered as either contaminated by clouds or otherwise unsuitable for further analysis.

After the computation of NDVI and BR_{BG} from radiances, the data are gridded on a regular latitude/longitude grid with a resolution of 0.0025°, which is about 280 m at this latitude, and thereby of similar magnitude as the resolution of OLCI. For each grid cell, the degree of WHY cover (WHYindex, I_{WHY}) is determined according to NDVI thresholds as follows:

If $N_V > N_V^{high}$, $I_{WHY} = 2$ (grid cell completely covered by plants)

If $N_V \geq N_V^{low}$, but $N_V < N_V^{high}$, $I_{WHY} = 1$ (grid cell partially covered or sparsely covered by plants)

All other cases: $I_{WHY} = 0$

where N_V^{high} and N_V^{low} denote two NDVI thresholds, as will be explained below.

If $BR_{BG} < 1.2$, I_{WHY} is set to -1, overriding other classification results. These gaps, i.e., $I_{WHY} = -1$, are filled in at a later stage (described in Sect. 2.5).

The NDVI thresholds are determined by identifying observations (1) completely covered and (2) completely free of WHY from the L1C data, by referring to NDVI from the MSI sensor, as shown in Figs. 2A and 2B. The OLCI spectra of a number of these observations were collected and averaged and are shown in Fig. 2C. From these, a set of synthetic spectra with varying fractions of WHY cover (f_{WHY}) was calculated by assuming linear mixing of radiances, in a fashion similar to (Villa et al., 2014). NDVI were computed from the mixed spectra and plotted as a function of f_{WHY}, as shown in Fig. 2D. The thresholds N_V^{high} and N_V^{low} were set at f_{WHY} = 0.75 and 0.5 and are indicated by dashed lines in Fig. 2. For the prototype algorithm, the thresholds were determined from data of September 1, 2022, giving N_V^{high} = 0.44 and 0.33 and N_V^{low} = 0.35 and 0.24 for S3A and S3B, respectively. Differences in calibration between the instruments on Sentinel-3A and -3B cause a difference in NDVI, therefore, the thresholds vary between the instruments.

The two upper panels of Figure 3 show the results for September 1, 2022.

https://doi.org/10.5194/egusphere-2026-403
Preprint. Discussion started: 10 February 2026

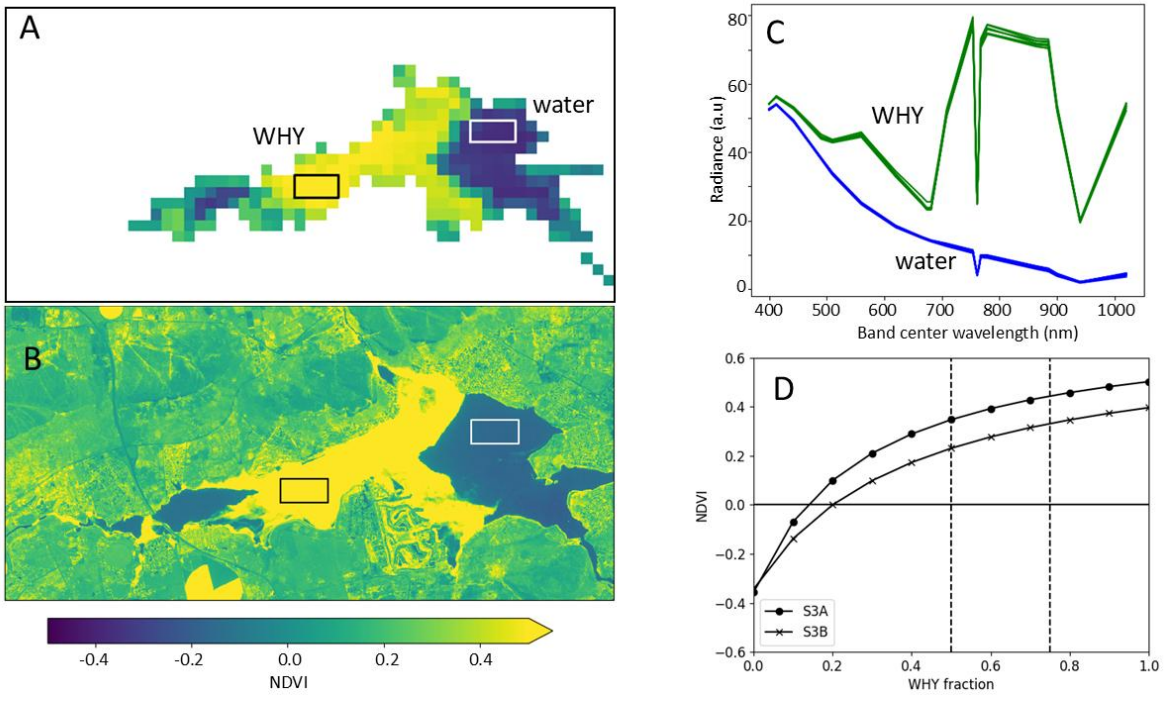

Figure 2. Steps in the determination of the WHY detection threshold. A. NDVI map from S3A OLCI data, 01/09/2022; B. NDVI from MSI on Sentinel-2 on 01/09/2022; C. OLCI L1C ToA radiance spectra from selected points within the white (water) and black (WHY) boxed regions indicated in panels A and B; D. NDVI dependence on WHY cover fraction of a satellite pixel for data from OLCI on S3A and S3B, 01/09/2022. See the text for details.

2.4. Merged WHYmaps

Maps of I_{WHY} from both OLCI instruments are merged into a single, daily data set. On most days, only one of the instruments viewed the scene, but roughly every week S3A views the Dam, 39 minutes after S3B. This happened, for example, on September 1, 5, 16, 20, 24, and 28, 2022. On these days, a merged WHYmap is created by following the scheme presented in Table 2. In general, if I_{WHY} is the same for both instruments, that value appears in the merged map; in most cases where the instruments disagree, the value is set to 1, unless one of the instruments yields I_{WHY} = -1. For example, if I_{WHY} of S3A equals 2 and for S3B I_{WHY} = -1, the merged value equals 2; but the merged value is set to 1 if S3B detects I_{WHY} = 1 or 0. The resulting merged map for September 1, 2022, can be seen in panel C of Fig. 3. To retain the traceability of the data, a bit-encoded source flag is created that indicates which OLCI instrument contributed to each merged grid cell: 1 and 2 for Sentinel-3A and 3B, respectively; 0 for neither, and 3 for both. Hence, the map in panel E of Fig. 3 shows that most of the observations were made by both instruments (source flag = 3, dark red color), with only a few scattered observations by S3A only (light blue) or S3B only (yellow).

https://doi.org/10.5194/egusphere-2026-403
Preprint. Discussion started: 10 February 2026

Table 2. Scheme for merging observations by the instruments on S3A and S3B. The combination of the value given in the top row with that in the left-most column gives the corresponding value in the white body of the table.

		I_{WHY} S3B			
	Classes	**0: no WHY**	**1: WHY-sparse**	**2: WHY - confident**	**-1: unknown /missing**
I_{WHY} S3A	**0**	0	1	1	0
	1	1	1	1	1
	2	1	1	2	2
	-1	0	1	2	-1

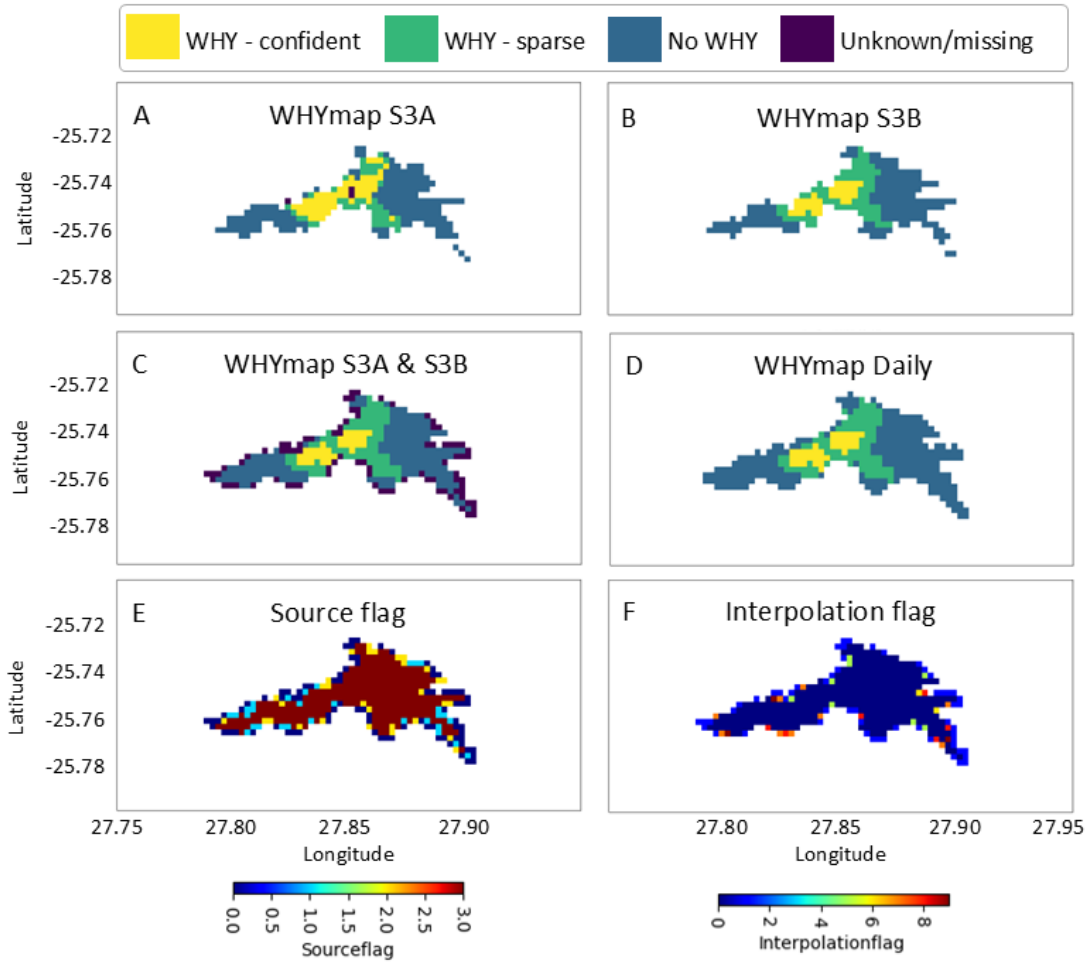

https://doi.org/10.5194/egusphere-2026-403
Preprint. Discussion started: 10 February 2026

Figure 3. WHY mapping product of September 1, 2022. A – WHYmap derived from Sentinel-3A; B – WHYmap derived from Sentinel-3B; C – WHYmap obtained by merging the results in panels A and B according to Table 2; D – Daily, gap-filled, merged WHYmap. E – WHYmap source flag; F – WHYmap interpolation flag. The colour bar for the upper four panels is shown at the top of the figure, whereas the colour bars for the lower panels are shown beneath the respective panel.

2.5. Gap-filling strategy

Any missing values (i.e., I_{WHY} = -1) remaining in the merged WHYmaps are interpolated by taking the most frequent value from neighboring grid cells. For each missing value in a WHYmap, an interpolation is performed according to the flowchart in Fig. 4. The process is shown exemplarily for the shaded gridcell at the center of the 3x3 kernel shown on the top row of Fig. 4: cell A. In the first step, the eight gridcells directly surrounding cell A of a missing value are evaluated (shaded cells in the second 3x3 square). If at least half (i.e., four or more) of those contain valid entries, the median of those entries is assumed to be the best approximation for cell A. If three or less neighboring entries are valid, the two neighboring time steps (at t-1 and t+1) are additionally evaluated. If this data set, shown schematically as the three overlapping 3x3 squares, contains more than six valid entries, the median of those data is used to fill cell A. If there are not enough valid entries, a climatological value is assumed for cell A. The climatology is the 28-day rolling median of a grid cell, considering valid entries only (I_{WHY} = 0, 1 or 2), according to:

$$\widetilde{I_{WHY}} = M(I_{WHY}(t = t - 14) \dots I_{WHY}(t = t + 14)) \quad (3)$$

where M denotes the median over the valid I_{WHY} values of a particular grid cell within the 28-day time period. At the edges of the time series (the first or last 14 days of a data set) an asymmetric rolling median is calculated as follows:

$$\widetilde{I_{WHY}} = M(I_{WHY}(t = t_0) \dots I_{WHY}(t = t + 14)) \quad (4)$$

or:

$$\widetilde{I_{WHY}} = M(I_{WHY}(t = t - 14) \dots I_{WHY}(t = t_{end})) \quad (5)$$

with t_0 and t_{end} denoting the first and last time step of the data set, respectively.

https://doi.org/10.5194/egusphere-2026-403
Preprint. Discussion started: 10 February 2026

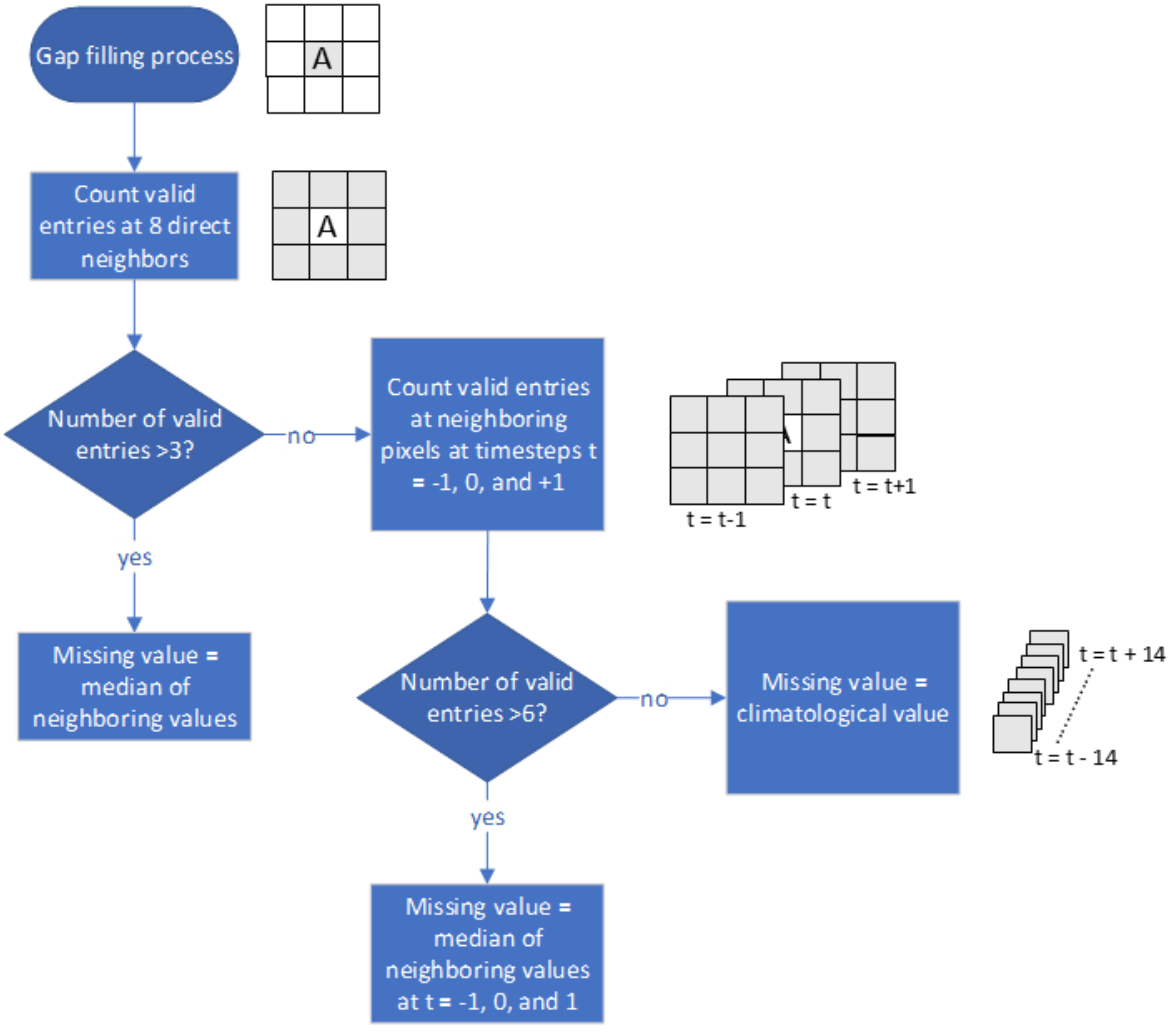

Figure 4. Flowchart of WHYmapping gap-filling process.

By applying the gap-filling process to each grid cell containing missing data, a gap-free set of WHYmaps is obtained at a daily frequency. The origin of the gap-filled value can be traced back by referring to the interpolation flag (panel F of Fig. 3). The flag encoding is as follows:

0 – no interpolation

1 – value from climatology

4-8 – median value of neighboring grid cells in same time step

6-18 – median value of neighboring grid cells in neighboring time steps

The values 2 and 3 are not used, whereas both types of neighboring interpolations may yield an interpolation flag of 6, 7, or 8.

https://doi.org/10.5194/egusphere-2026-403
Preprint. Discussion started: 10 February 2026

3. Results

3.1. Daily WHYmaps from OLCI

The WHYmapping product contains six variables, as displayed exemplarily for September 1, 2022 in Fig. 3, when both OLCI instruments observed the Dam. The top two panels show WHYmaps derived from the instrument on S3A (A, left), and S3B (B, right). The location of the plants is similar in both panels, but S3A yields more grid cells classified as "WHY – confident" compared to S3B. Panel C shows the merged product, with values missing in both instruments classified as "unknown/missing". These gaps are filled in the final algorithm step, of which the resulting "WHYmap Daily" is shown in panel D. The lower left panel (E) presents the source flag, which shows which instrument observed the particular grid cell. The meaning of the flags is: 1- S3A only; 2 – S3B only; 3 – S3A and S3B; 0 – neither instrument. The flag in panel F provides information on the interpolation method, as described above.

On September 1, only few grid cells required interpolation, but on October 4, 2022, a large section in the western part of the Dam was classified as "unknown", because the BR_{BG} did not exceed the threshold, indicating cloud contamination. Figure 6 shows the WHYmap derived from S3B (panel A) and the merged map (C) with a large number of gaps. Applying the interpolation algorithm yields the map in panel E. The algorithm filled some of the smaller gaps with data from neighbouring grid cells, but not the centre of the large gap in the western part of the Dam. The merged WHYmaps of the days directly preceding and following October 4 contained valid data over most of the Dam (panels B and D), hence, the remaining gaps were interpolated using the nearest neighbours in time, instead of reverting to the climatology. This can be reconstructed based on the interpolation map shown in panel F: the region gap-filled in this fashion has an interpolation flag of 9 or higher (panel F), as opposed to a flag of 1, which indicates the use of climatological values.

https://doi.org/10.5194/egusphere-2026-403
Preprint. Discussion started: 10 February 2026

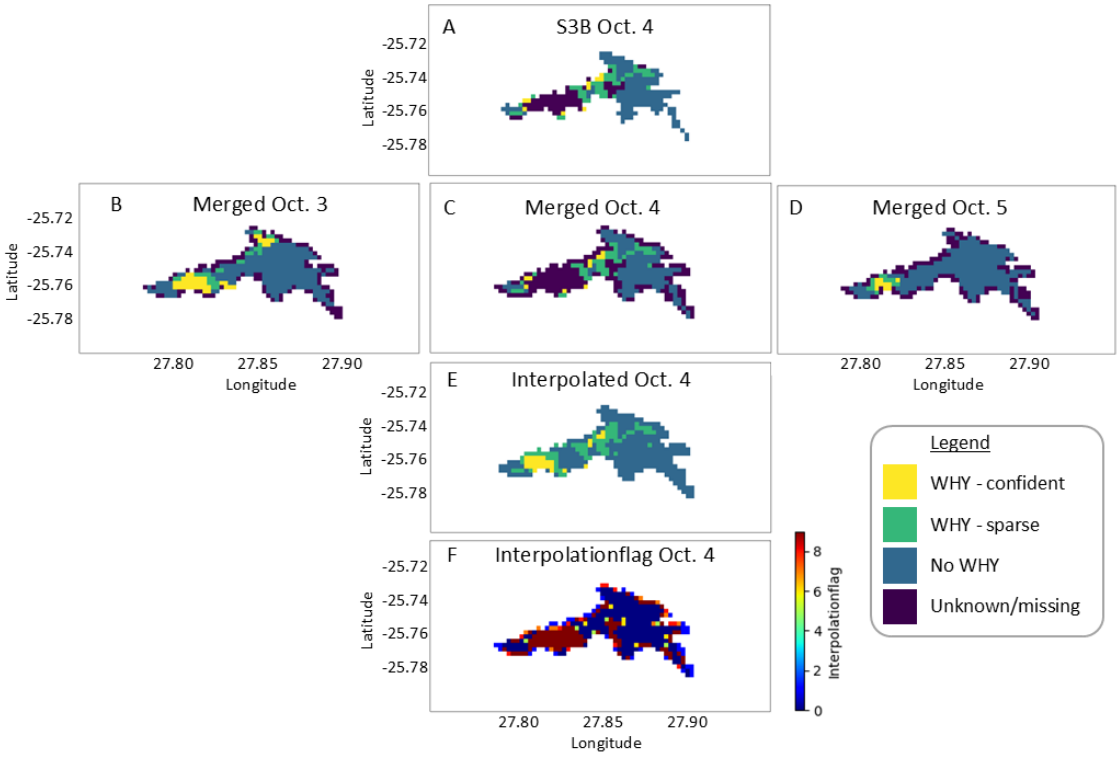

Figure 5. Illustration of the gap-filling method for October 4, 2022. The WHYmap derived from Sentinel-3B data is shown in panel A; merged WHYmaps of Oct. 3-5 are shown in panels B, C, and D; the gap-filled daily WHYmap, and the corresponding interpolation flag for Oct. 4 are shown in panels E and F, respectively.

3.2. Evaluating the gap-filling strategy

The gap-filling method was evaluated by a leave-one-out type of analysis of a selection of the data set. This analysis entails the removal of 1, 2 or 3 daily maps from a series of five, applying the gap-filling algorithm to the missing data, and comparing the results with the original (reference) time series. The results are shown for three such analyses in Figure 6. In the first column, daily (gap-filled) WHYmaps of the reference data set are shown for (top to bottom) August 12-16, 2022. A large WHY patch is seen in the northern section of the Dam on August 12, which has increased its extent in a southward direction on the following day. On August 14, the plants cover an appreciably smaller area in the East of the Dam on account of wind (as shown in Fig. A6 in the appendix). In the following two days, the patch is seen to increase its surface area, reaching the northernmost section of the Dam again on August 16. This short time series clearly illustrates the spatio-temporal variability of the aquatic vegetation.

https://doi.org/10.5194/egusphere-2026-403
Preprint. Discussion started: 10 February 2026

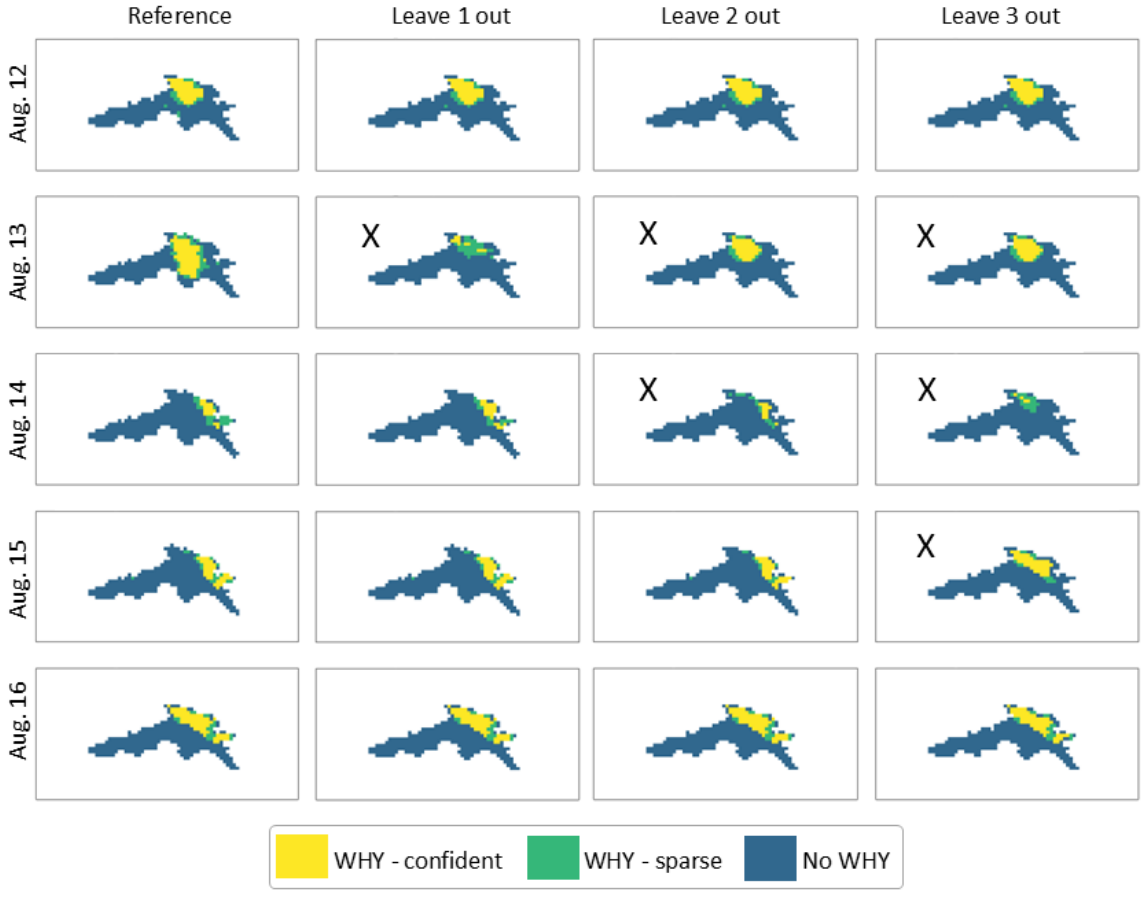

Figure 6. Results of the leave-one-out type of analysis used to test the gap-filling WHYmapping algorithm. Each column shows the gap-filled daily WHYmaps for August 12-16 resulting from: (first column) the reference data set; (second) the data set in which August 13 was left out; (third) the data set in which August 13-14 were left out; and (fourth) the data set in which August 13-15 were left out. Data left out (and replaced using the gap-filling algorithm) are marked by an X.

The second column of Fig. 6 shows the series of maps obtained when the WHYmap of August 13 (marked with an X) is replaced by missing values and subsequently gap-filled using the WHYmapping algorithm. In this series, the gap-filling algorithm creates a map from the median of neighboring grid cells on August 12 and 14. The big change in spatial distribution that occurred between August 13 and 14 causes the algorithm to misrepresent the situation on August 13, leading to a difference in coverage fraction of 20%, or 3.8 km^2 (Table 3).

The third column shows the series of maps that result when a similar method is performed on a time series where both August 13 and 14 are replaced by missing values. The WHYmap of August 13 is very similar to that of the preceding time step, as the gap-filling algorithm used the merged WHYmap of August 12 to reconstruct the missing data. On August 14, most of the missing data are replaced using the nearest-neighbour method (causing a high degree of similarity with August

https://doi.org/10.5194/egusphere-2026-403
Preprint. Discussion started: 10 February 2026

15), but a number of grid cells near the coastline are assigned values from the climatology, as they are missing in the merged WHYmap of August 15.

The fourth column shows the resulting maps when the data of August 13-15 are removed. Again, the nearest-neighbour strategy employed for the WHYmaps of August 13 and 15 can be clearly recognized by their similarity with WHYmaps of neighbouring time steps. The WHYmap of August 14, however, is completely taken from the climatology, as nearest neighbours are missing. The degree of agreement with the reference map is high, because the reference WHYmap of August 14 is similar to the climatology.

The results of the complete leave-one-out analysis are summarized in Table 3, which presents the total WHY coverage of the Dam (sparse and confident classifications) for the days August 13, 14 and 15 for each of the leave-one-out tests, with the deviation from the reference (second row) given in brackets. As expected, the algorithm generally works better if neighbouring maps (or the climatology) are similar to the missing data. This is evidenced by the lower performance of the gap-filling algorithm on Aug. 13 (Table 3, second column) on account of the low similarity between the WHY coverage on that day compared to Aug. 14 and the climatology. In contrast, leaving out one day of data causes the fractional coverage on Aug. 14 and 15 to be overestimated by less than 10% (rows 3, 4 and 5). Leaving out more days only causes a discrepancy higher than 10% for August 14 (light blue box in Table 3). As mentioned, the good agreement on August 14 in the leave-three-out series (less than 1 km^2 difference with the reference) is due to the somewhat coincidental high similarity between the climatology and the observation.

Table 3. Total WHY coverage (in km^2; total Dam area: 19 km^2) in the interpolated WHYmaps created within the leave-one-out type analysis. Values in parentheses denote the deviation from the reference maps (second row); deviations larger than 10% of Dam area are shaded light red or light blue (for smaller and larger values, respectively) and a darker shade of red for the deviations larger than 20% of Dam area.

Leave-out scheme	August 13	August 14	August 15
Reference	6.65	2.66	3.23
Aug. 13 left out	2.85 (-3.80)	2.47 (-0.19)	3.23 (+0.00)
Aug. 14 left out	6.46 (-0.19)	4.18 (+1.52)	2.85 (-0.38)
Aug. 15 left out	6.65 (+0.00)	2.28 (-0.38)	3.80 (+0.57)
Aug. 13-14 left out	3.80 (-2.85)	1.71 (-0.95)	2.85 (-0.38)
Aug. 13 and 15 left out	2.85 (-3.80)	2.09 (-0.57)	3.80 (+0.57)
Aug. 14-15 left out	6.46 (-0.19)	5.89 (+3.23)	3.61 (+0.38)
Aug. 13-15 left out	3.80 (-2.85)	1.71 (-0.95)	3.61 (+0.38)

https://doi.org/10.5194/egusphere-2026-403
Preprint. Discussion started: 10 February 2026

3.3. Use case: Monitoring of WHY in Hartbeespoortdam Reservoir

The daily WHYmaps can be used to monitor WHY proliferation, as shown in Fig. 8. But to illustrate the added value of the proposed interpolation scheme, we first present the time series of merged (not yet interpolated) WHYmaps in Fig. 7. The main panel depicts a stacked bar chart containing the fraction of grid cells classified as "WHY sparse" (green), or "WHY confident" (yellow). Grey bars indicate days without Sentinel-3 overpasses. In the upper panel, the fraction of grid boxes with valid I_{WHY} (between 0 and 2) is shown as a black line. For reference, the grey bars showing days with no overpasses extend into the upper panel. According to Fig. 7, the fraction of the Dam covered by WHY varies appreciably throughout the year: the time series shows a first clear peak in September 2022, followed by a period of high variability and three strong peaks in January, March and April 2023. Between May and October 2023, the Dam is mostly free of WHY, after which the coverage starts to increase again to about 40% of the water surface at the end of the year.

The grey bars indicate that there are roughly 3-4 days every month on which neither S3A nor S3B views the scene. These days (naturally) coincide with a fraction of 0% valid observations (top panel, black line). But there are an appreciable number of data gaps that do not coincide with observation-less days, for example in February 2023 – apparently in the middle of the peak WHY season. On these days, the lack of observations is due to cloud cover. A check of MSI images in that time period confirms that thick clouds regularly obscure the view of the Dam partly or completly. For this reason, the time series displays large gaps from Feb. 8-15, 17-19; and only few valid observations on Feb. 16, 22 and 23 (see also Figs. A1-A4 in Appendix A).

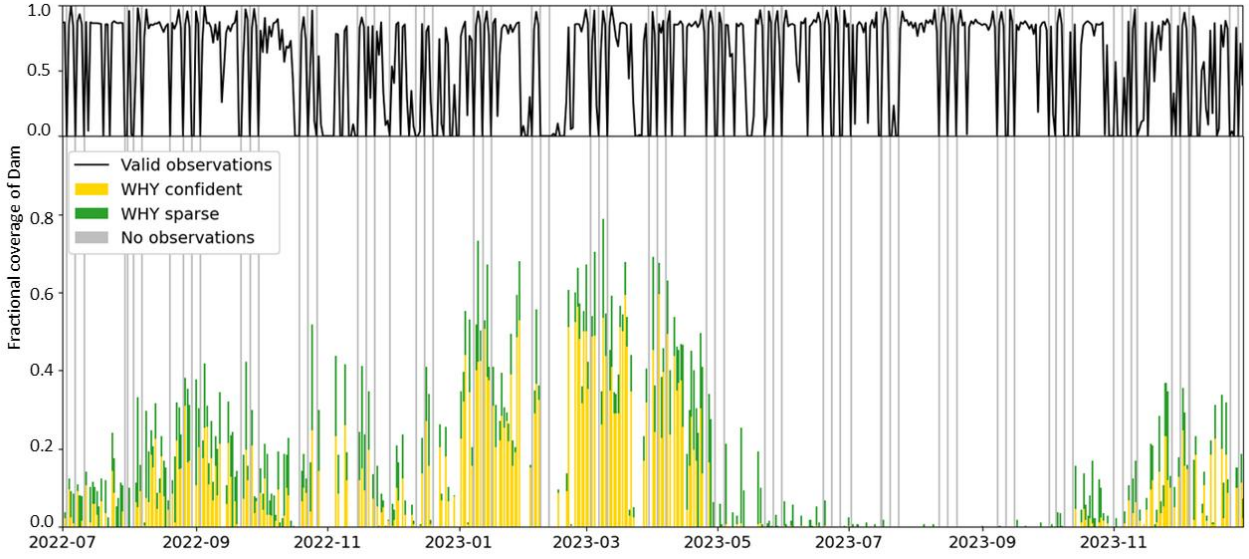

Figure 7. Observed fraction of the Dam covered by aquatic plants for days between July 1, 2022 and December 31, 2023. Lower panel: stacked barchart depicting the fractional coverage by WHY (yellow) and sparse WHY (green). Grey bars indicate days without Sentinel-3 overpasses. Upper panel: fraction of grid cells with valid observations (black line) and days without satellite overpasses (grey bars).

https://doi.org/10.5194/egusphere-2026-403
Preprint. Discussion started: 10 February 2026

The WHYmapping interpolation scheme was developed to create a consistent time series with daily resolution, hence without the gaps featured in Fig. 7. The stacked bar chart in Fig. 8 depicts the time series obtained by plotting the fraction of WHY determined from the daily interpolated WHYmaps. In general, as expected, the coverage of both sparse and confident WHY increased due to the gap-filling: after interpolation, the number of days with WHYmaps increased from 353 to 549 after interpolation (56% increase). Yet the main features – the peaks in the first half of the time series, the near-zero fractions from May-October 2023, and the peak at the end of the time series – remain clearly visible, and more smooth. In particular, the data gap in February 2023 appears to be consistently filled, and the number of days with WHYmaps increased from 9 to 28 after application of the interpolation scheme. How the algorithm handled the time period February 6-25 can be seen in the WHYmaps and flags presented in Figs. A1-A4 in Appendix A.

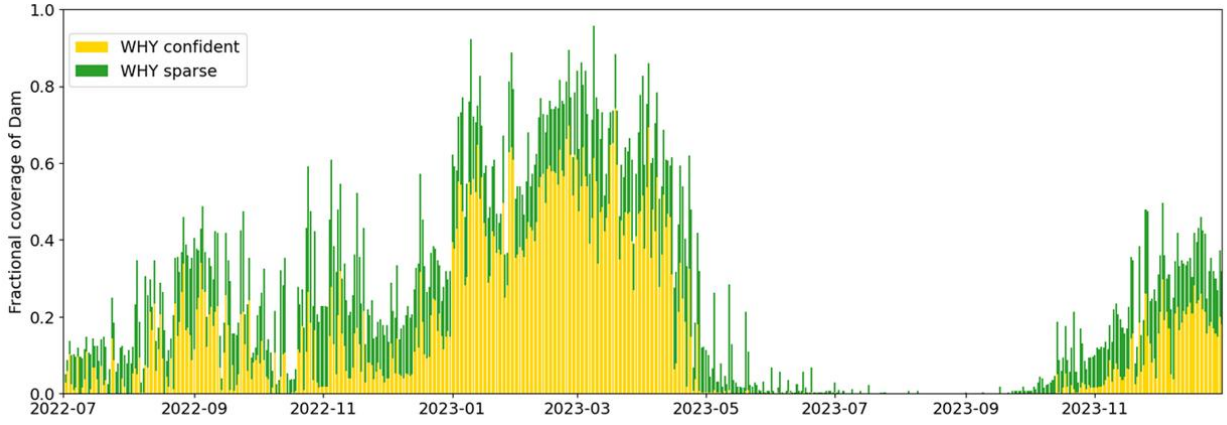

Figure 8. Interpolated daily fraction of the Dam covered WHY (yellow) and sparse WHY (green) for days between July 1, 2022 and December 31, 2023.

The pattern of WHY cover in Fig. 8 follows a seasonal cycle, peaking at the end of the warm wet season (October-April). Daytime temperatures are between 20°C and 30°C on average during this season, which is optimal for WHY growth. The rapid decline in floating vegetation cover in May might be due to the cold night temperatures, which regularly drop below 10°C, under which WHY ceases to grow (Coetzee et al., 2017; Wilson et al., 2005).

4. Discussion

The high variability of WHY occurrence makes daily monitoring a requirement when assessing prevention and removal strategies. Yet, despite numerous studies using satellite remote sensing to detect WHY, an algorithm to derive daily maps for systematic monitoring of WHY cover has not yet been presented. Our WHYmapping algorithm addresses this need and can be used by water managers to assess the effectiveness of management strategies or by scientists to investigate causes and effects of WHY in a systematic fashion.

https://doi.org/10.5194/egusphere-2026-403
Preprint. Discussion started: 10 February 2026

The WHYmaps created by applying thresholds to NDVI data from OLCI on Sentinel-3A and 3B contain gaps; even after merging the data of both platforms. The gaps are due to missing observations (grey lines in Fig. 7) and to data points flagged as possibly contaminated by clouds. To fill these gaps, a strategy is adopted here that is similar to the post-processing step in the TROPOMI surface albedo algorithm. The step makes use of nearby "donor cells" to fill gaps caused by persistent cloud cover (Tilstra et al., 2024). Applying the gap-filling algorithm to WHYmaps leads to a more complete, consistent timeseries, as shown in Fig. 8. From the evaluation of the gap-filling algorithm in Section 3.2 we find that gap-filled maps are in good agreement with the actual observations if there are no sudden changes in WHY cover patterns – as may be expected for an algorithm that relies on continuity. A more accurate gap-filling may be achieved by explicitly modelling the evolution and propagation of floating vegetation, e.g. by taking into account drivers affecting the position of WHY (water currents, wind speed and direction) and parameters affecting growth (temperature, nutrient concentration) (Coetzee et al., 2017). The development of such a process-based (hydrodynamical and biochemical/physical) model is not within the scope of this study; however, the timeseries created by our algorithm may, when correlated with abovementioned parameters, aid the calibration or boundary condition definition of such a model. This could support the identification of drivers and enable the parameterization of their effects, thereby laying the foundations for future process-based modelling efforts.

The main patterns of WHY cover on the Dam can be explained by the effects of temperature on plant growth (Section 3.3), in agreement with previous observations (Dersseh et al., 2020; Janssens et al., 2022; Kleinschroth et al., 2021). But on a shorter timescale WHY and other floating aquatic vegetation are strongly affected by wind and currents. Moreover, removal actions, such as the introduction of specific herbivores or spraying of herbicides affect WHY strongly and may cause sudden changes in the pattern. Some of these effects appear as high-frequency variations in the time series. The effects of the wind direction change between August 13 and 14 is clearly seen in the first column of Fig. 6: whereas WHY was detected on the North and center of the Dam on August 12 and 13, the wind had pushed the plants to the eastern shore by the time the satellite passed over on the morning of August 14.

The time series of daily WHYmaps of the presented prototype algorithm currently spans eighteen months. The algorithm is relatively light-weight and can be easily applied to longer time series with larger datasets. One limitation at present is the manual determination of NDVI thresholds, which relies on expert knowledge. This part of the algorithm should be automated before it can be applied on a global scale.

The prototype algorithm uses Level-1C data to be independent of the Level-2 quality filters, which are considered too conservative for our purposes, particularly the cloud filter. This means that TOA radiances, uncorrected for atmospheric effects, are used to calculate the spectral indices (NDVI and BR_{BG}) and their respective thresholds. As the indices are the ratio of radiances in two wavelength bands, the effects of viewing and solar angles essentially cancel out; but this is not always the case for atmospheric effects, such as a large aerosol load (Huang et al., 2021). A potential improvement to the algorithm could be the inclusion of atmospheric correction (AC) as a first step.

While AC might enhance the consistency of WHY detection thresholds between Sentinel-3A and Sentinel-3B, its impact on the overall results is not guaranteed and may vary depending on the viewing-illumination geometry and atmospheric load of

https://doi.org/10.5194/egusphere-2026-403
Preprint. Discussion started: 10 February 2026

aerosols. Nevertheless, the use of TOA radiance remains appealing due to its simplicity, computational efficiency, and global availability, making it particularly suitable for scalable applications and rapid prototyping.

The introduction of the BR_{BG} threshold allows the removal of thick clouds that have an appreciable effect on observed radiances. Pixels identified as cloudy by this threshold are assigned a fill value. Thin or partial clouds may not be detected in this manner, which is intentional, as the strong spectral response from floating plants makes it possible to identify them even under mildly cloudy conditions, increasing the number of valid observations appreciably.

During a field visit in October, 2022, it became apparent that the Dam was covered in plants – but only a fraction of those were WHY. The plant covering most of the Dam on that day, giant salvinia (*Salvinia molesta*), could be observed in the satellite images as well as WHY itself, therefore the WHYmapping algorithm can be considered useful to monitor other floating aquatic species as well. Nevertheless, there are reasons to investigate both species separately, and we are exploring the possibility of using Sentinel-2 and -3 data to discriminate between WHY and giant salvinia.

We are currently applying the WHYmapping algorithm to the complete OLCI time series (2016-2025) to investigate how WHY reacts to herbicide spraying on the Dam. The time series of WHYmaps will also allow a systematic study of various management strategies and environmental effects on WHY.

5. Concluding remarks

The presented algorithm offers a simple, computationally efficient, and globally applicable solution by utilizing Top-of-Atmosphere (TOA) reflectance data to map floating vegetation. The novel interpolation scheme increases the number of observation days by >50%. The algorithm's adaptability to different geographic regions is supported by its use of satellite-derived thresholds; however, this process still relies on expert input. Automating threshold selection will be essential for scaling the method to broader applications and enhancing its usability across diverse environments.

By running the algorithm on a cloud-computing server with direct access to satellite data, such as the EOAFRICA Innovation Platform or the Copernicus Data Space Ecosystem (https://dataspace.copernicus.eu/), users do not require expensive hard- or software, or even large-bandwidth internet connections. This allows the use of the algorithm by scientists in the tropical and sub-tropical regions that suffer most from water hyacinth invasions, and who might have limited access to computing power and/or funding.

Appendix A

The following four figures (A1-A4) show the timeseries of WHYmaps to illustrate how the interpolation (gap-filling) algorithm handles missing data over a large number (>3) of consecutive days. In the first column, the merged WHYmaps (data from both Sentinel-3 platforms) are shown for five consecutive days per figure. These contain gaps indicated in dark blue. The second column shows the daily WHYmaps, where missing data have been replaced by the gap-filling algorithm.

https://doi.org/10.5194/egusphere-2026-403
Preprint. Discussion started: 10 February 2026

The third column displays the sourceflag, which encodes the source of the values in the merged WHYmap: 1, 2 and 3 indicate satellite data as the source, whereas a flag of 0 indicates no overpass (see Sect. 3.1 for details). For example, on Feb. 7, the sourceflag indicates that all valid data in the merged WHYmap comes from Sentinel-3A (sourceflag = 1); on Feb. 8, there was no satellite overpass (sourceflag = 0) and on Feb. 9, data came from Sentinel-3B (sourceflag = 2). Note that due to the size of the OLCI footprint, grid cells along the coastline are often not observed. The fourth column shows the interpolation flag, which indicates how many grid cells are used for gap-filling. The value ranges from 0 (no gap-filling) to 1 (gap-filling from climatology), 4-8 (gap-filling by nearest neighbors in place) and 6-16 (gap-filling by nearest neighbors in space and time). The data missing on Feb. 8 was mostly replaced by data from nearest neighbors in space and time, as indicated by the interpolation flag of 9 and higher. On Feb. 9, the whole map was filled from the climatology, as no nearest neighbors were available.

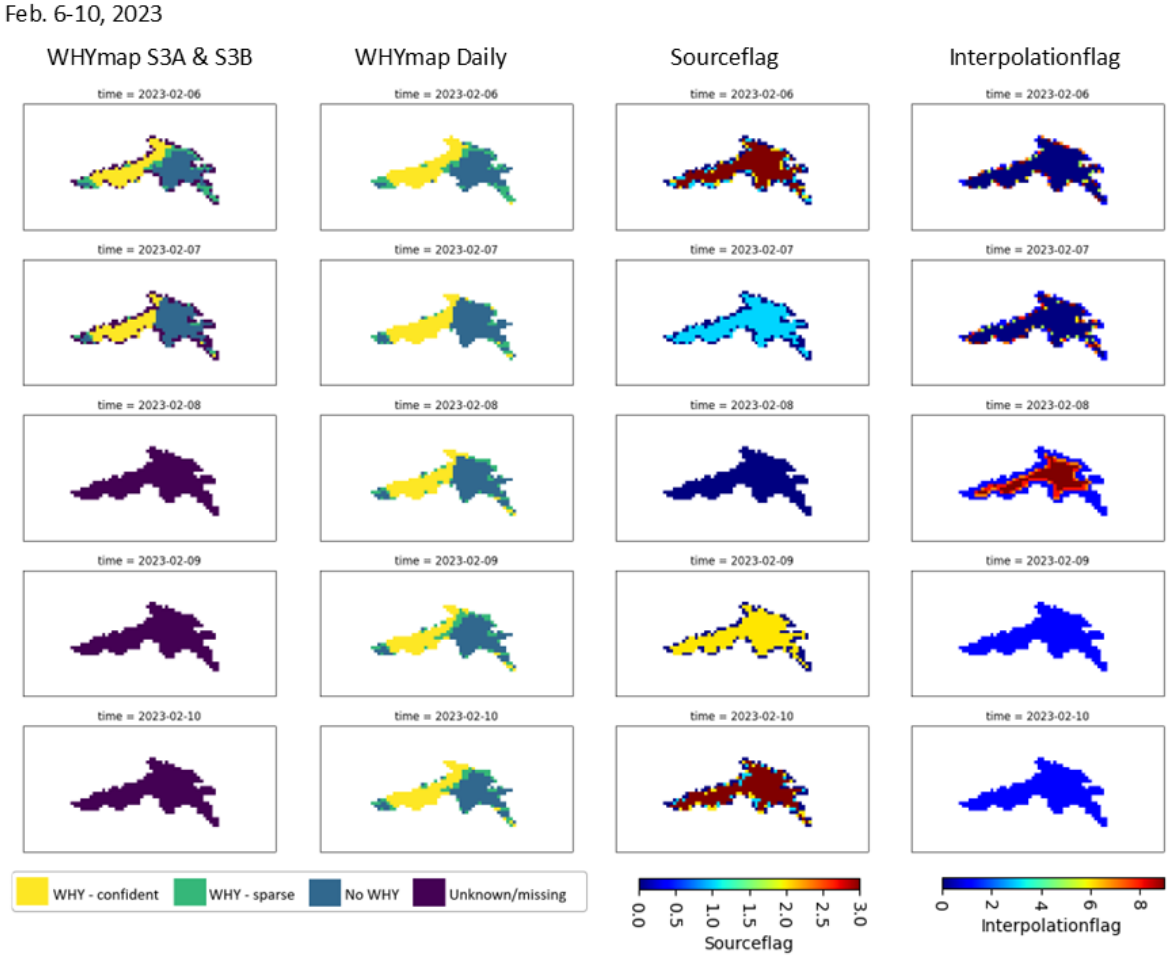

Figure A1. Timeseries of WHYmaps for (top to bottom) Feb. 6-10, 2023. From left to right, columns show: merged WHYmaps (observations of S3A and S3B combined); daily WHYmaps (after interpolation of missing values); map of sourceflags; map of interpolationflags.

https://doi.org/10.5194/egusphere-2026-403
Preprint. Discussion started: 10 February 2026

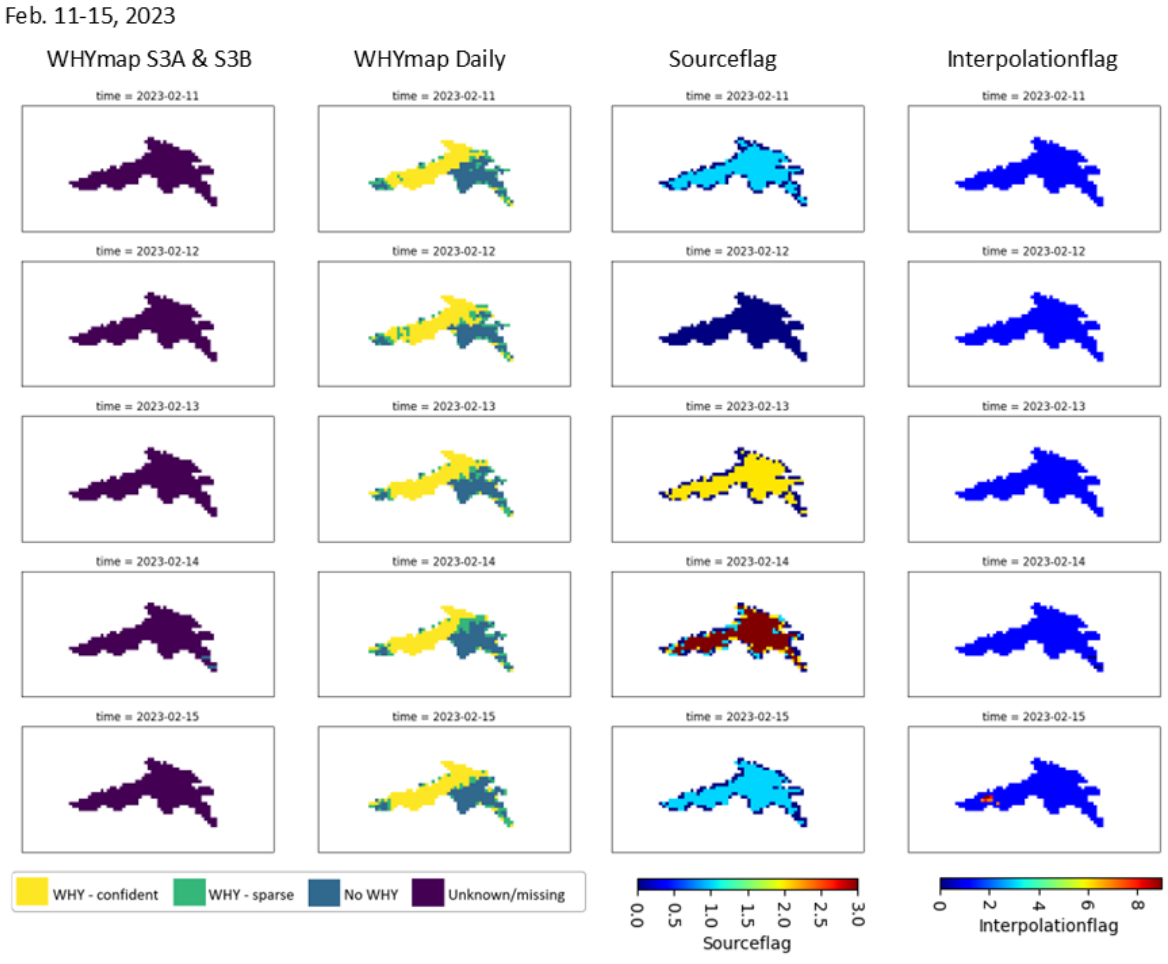

Figure A2. As Fig. A1, but for Feb. 11-15, 2023.

https://doi.org/10.5194/egusphere-2026-403
Preprint. Discussion started: 10 February 2026

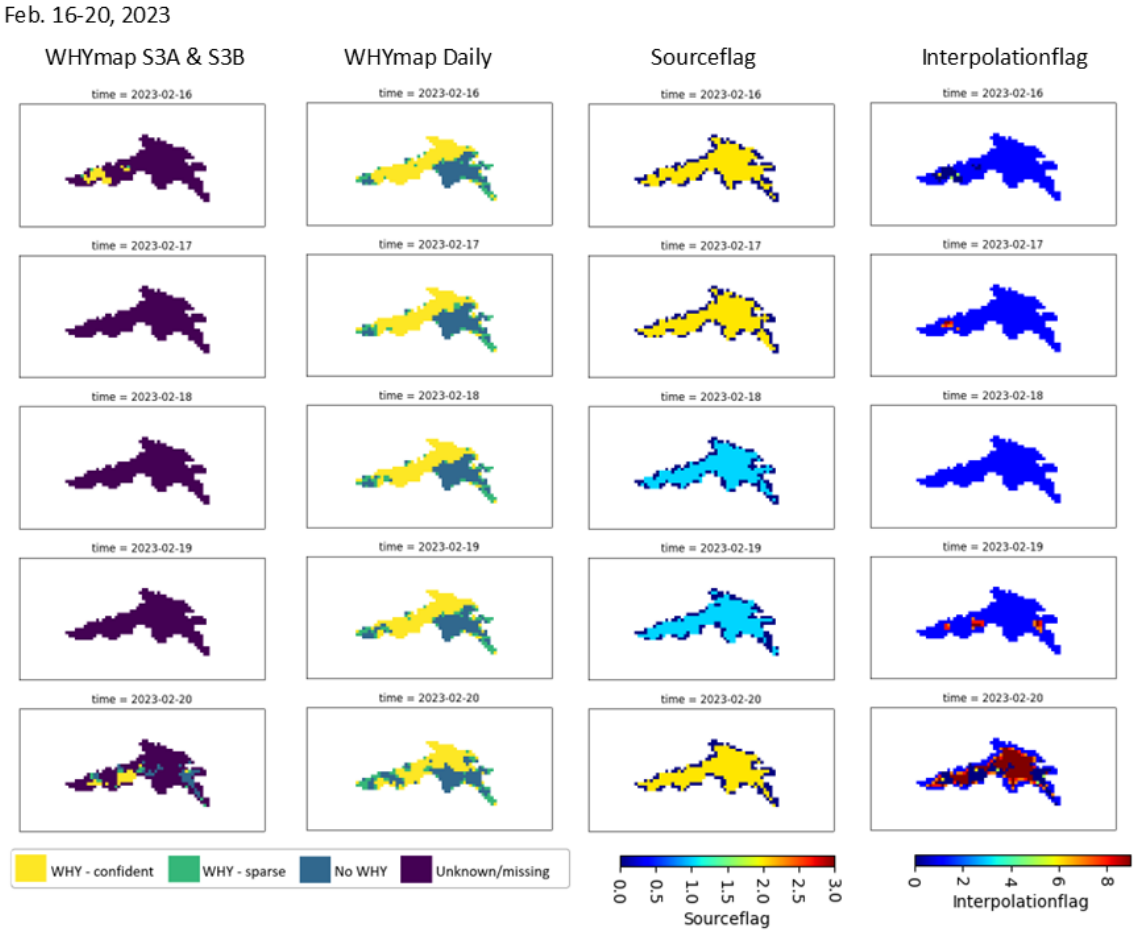

Figure A3. As Fig. A1, but for Feb. 16-20, 2023.

https://doi.org/10.5194/egusphere-2026-403
Preprint. Discussion started: 10 February 2026

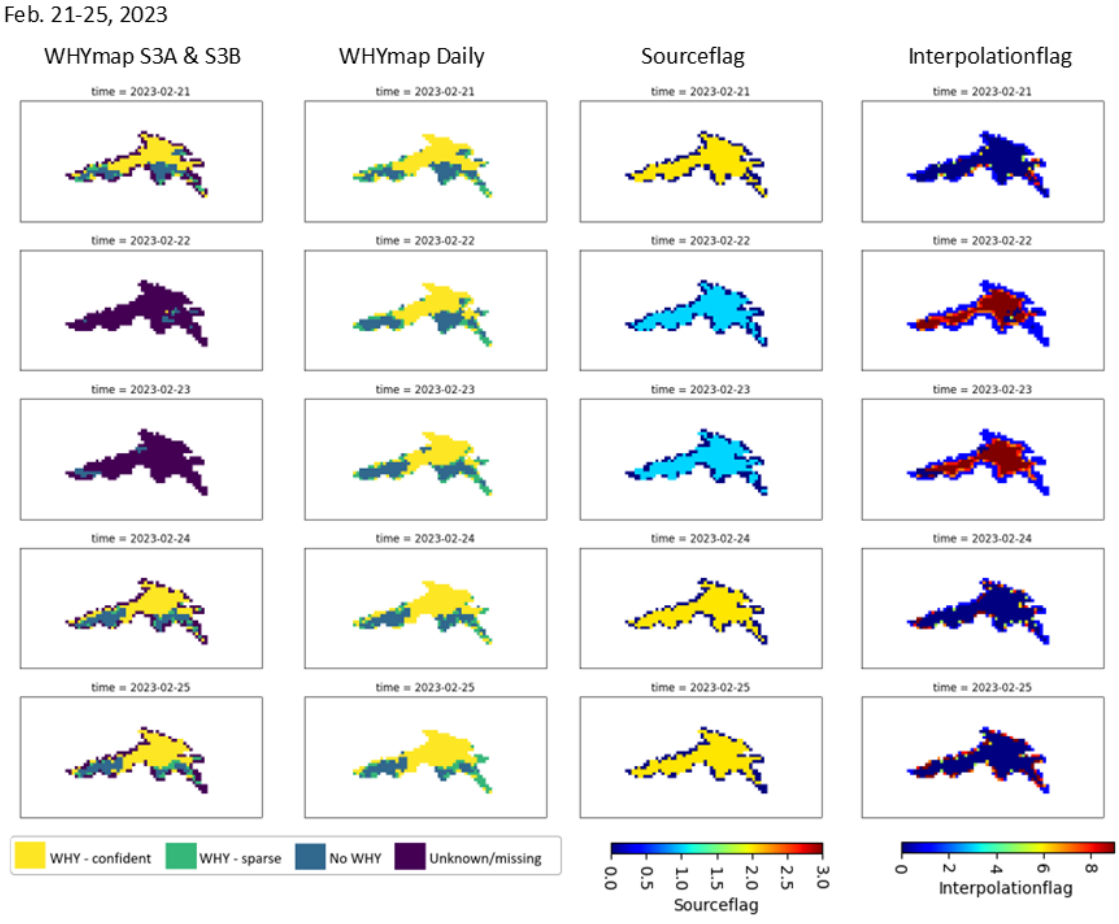

Figure A4. As Fig. A1, but for Feb. 21-25, 2023.

Code and data availability

The WHYmapping algorithm code and code used to produce figures will will be published on Zenodo, along with the data produced within the study, after final revision of the paper. Sentinel-2 MSI and Sentinel-3 OLCI radiance data are freely available from various platforms; for this study, data were retrieved from Copernicus' WEkEO platform (www.wekeo.copernicus.eu).

Author contributions

M.P.d.V. designed the study, research execution by M.P.d.V., C.S., K.H.T., and advice from T.D. and S.S., drafting of manuscript by M.P.d.V. and review by all.

https://doi.org/10.5194/egusphere-2026-403
Preprint. Discussion started: 10 February 2026

Competing interests

The authors declare that there is no conflict of interest.

Acknowledgements

The presented study was conducted within the African Framework for Research Innovation, Communities, and Applications in Earth Observation (EO AFRICA), funded by the European Space Agency (ESA). Code development and calculations were performed on the ITC Geospatial Computing Platform (CRIB). We are grateful to Serkan Girgin for expert assistance with the CRIB and Finn Münch for help with the visualisation of MSI data.

Review statement

The review statement will be added by Copernicus Publications listing the handling editor as well as all contributing referees according to their status anonymous or identified.

References

Albano Pérez, E., Coetzee, J. A., Ruiz Téllez, T., and Hill, M. P.: A first report of water hyacinth (Eichhornia crassipes) soil seed banks in South Africa, South African Journal of Botany, 77, 795–800, https://doi.org/10.1016/j.sajb.2011.03.009, 2011.

Bayable, G., Cai, J., Mekonnen, M., Legesse, S. A., Ishikawa, K., Imamura, H., and Kuwahara, V. S.: Detection of Water Hyacinth (Eichhornia crassipes) in Lake Tana, Ethiopia, Using Machine Learning Algorithms, Water, 15, 880, https://doi.org/10.3390/w15050880, 2023.

Cavalli, R. M., Laneve, G., Fusilli, L., Pignatti, S., and Santini, F.: Remote sensing water observation for supporting Lake Victoria weed management, Journal of Environmental Management, 90, 2199–2211, https://doi.org/10.1016/j.jenvman.2007.07.036, 2009.

Cheruiyot, E. K., Mito, C., Menenti, M., Gorte, B., Koenders, R., and Akdim, N.: Evaluating MERIS-Based Aquatic Vegetation Mapping in Lake Victoria, Remote Sensing, 6, 7762–7782, https://doi.org/10.3390/rs6087762, 2014.

Coetzee, J. A. and Hill, M. P.: The role of eutrophication in the biological control of water hyacinth, Eichhornia crassipes, in South Africa, BioControl, 57, 247–261, https://doi.org/10.1007/s10526-011-9426-y, 2012.

Coetzee, J. A., Hill, M. P., Ruiz-Téllez, T., Starfinger, U., and Brunel, S.: Monographs on invasive plants in Europe N° 2: Eichhornia crassipes (Mart.) Solms, Botany Letters, 164, 303–326, https://doi.org/10.1080/23818107.2017.1381041, 2017.

Datta, A., Maharaj, S., Prabhu, G. N., Bhowmik, D., Marino, A., Akbari, V., Rupavatharam, S., Sujeetha, J. A. R. P., Anantrao, G. G., Poduvattil, V. K., Kumar, S., and Kleczkowski, A.: Monitoring the Spread of Water Hyacinth (Pontederia crassipes): Challenges and Future Developments, Frontiers in Ecology and Evolution, 9, 6, https://doi.org/10.3389/fevo.2021.631338, 2021.

https://doi.org/10.5194/egusphere-2026-403
Preprint. Discussion started: 10 February 2026

Dersseh, M. G., Tilahun, S. A., Worqlul, A. W., Moges, M. A., Abebe, W. B., Mhiret, D. A., and Melesse, A. M.: Spatial and Temporal Dynamics of Water Hyacinth and Its Linkage with Lake-Level Fluctuation: Lake Tana, a Sub-Humid Region of the Ethiopian Highlands, Water, 12, 1435, https://doi.org/10.3390/w12051435, 2020.

Donlon, C., Berruti, B., Buongiorno, A., Ferreira, M.-H., Féménias, P., Frerick, J., Goryl, P., Klein, U., Laur, H., Mavrocordatos, C., Nieke, J., Rebhan, H., Seitz, B., Stroede, J., and Sciarra, R.: The Global Monitoring for Environment and Security (GMES) Sentinel-3 mission, Remote Sensing of Environment, 120, 37–57, https://doi.org/10.1016/j.rse.2011.07.024, 2012.

Drusch, M., Del Bello, U., Carlier, S., Colin, O., Fernandez, V., Gascon, F., Hoersch, B., Isola, C., Laberinti, P., Martimort, P., Meygret, A., Spoto, F., Sy, O., Marchese, F., and Bargellini, P.: Sentinel-2: ESA's Optical High-Resolution Mission for GMES Operational Services, Remote Sensing of Environment, 120, 25–36, https://doi.org/10.1016/j.rse.2011.11.026, 2012.

Fusilli, L., Collins, M. O., Laneve, G., Palombo, A., Pignatti, S., and Santini, F.: Assessment of the abnormal growth of floating macrophytes in Winam Gulf (Kenya) by using MODIS imagery time series, International Journal of Applied Earth Observation and Geoinformation, 20, 33–41, https://doi.org/10.1016/j.jag.2011.09.002, 2013.

Gbetkom, P. G., Crétaux, J.-F., Tchilibou, M., Carret, A., Delhoume, M., Bergé-Nguyen, M., and Sylvestre, F.: Lake Chad vegetation cover and surface water variations in response to rainfall fluctuations under recent climate conditions (2000−2020), Science of The Total Environment, 857, 159302, https://doi.org/10.1016/j.scitotenv.2022.159302, 2023.

Güereña, D., Neufeldt, H., Berazneva, J., and Duby, S.: Water hyacinth control in Lake Victoria: Transforming an ecological catastrophe into economic, social, and environmental benefits, Sustainable Production and Consumption, 3, 59–69, https://doi.org/10.1016/j.spc.2015.06.003, 2015.

Harun, I., Pushiri, H., Amirul-Aiman, A. J., and Zulkeflee, Z.: Invasive Water Hyacinth: Ecology, Impacts and Prospects for the Rural Economy, Plants, 10, 1613, https://doi.org/10.3390/plants10081613, 2021.

Huang, S., Tang, L., Hupy, J. P., Wang, Y., and Shao, G.: A commentary review on the use of normalized difference vegetation index (NDVI) in the era of popular remote sensing, J. For. Res., 32, 1–6, https://doi.org/10.1007/s11676-020-01155-1, 2021.

Janssens, N., Schreyers, L., Biermann, L., Ploeg, M. van der, Bui, T.-K. L., and Emmerik, T. van: Rivers running green: water hyacinth invasion monitored from space, Environ. Res. Lett., 17, 044069, https://doi.org/10.1088/1748-9326/ac52ca, 2022.

Jenny, J.-P., Anneville, O., Arnaud, F., Baulaz, Y., Bouffard, D., Domaizon, I., Bocaniov, S. A., Chèvre, N., Dittrich, M., Dorioz, J.-M., Dunlop, E. S., Dur, G., Guillard, J., Guinaldo, T., Jacquet, S., Jamoneau, A., Jawed, Z., Jeppesen, E., Krantzberg, G., Lenters, J., Leoni, B., Meybeck, M., Nava, V., Nõges, T., Nõges, P., Patelli, M., Pebbles, V., Perga, M.-E., Rasconi, S., Ruetz, C. R., Rudstam, L., Salmaso, N., Sapna, S., Straile, D., Tammeorg, O., Twiss, M. R., Uzarski, D. G., Ventelä, A.-M., Vincent, W. F., Wilhelm, S. W., Wängberg, S.-Å., and Weyhenmeyer, G. A.: Scientists' Warning to Humanity: Rapid degradation of the world's large lakes, Journal of Great Lakes Research, 46, 686–702, https://doi.org/10.1016/j.jglr.2020.05.006, 2020.

Jones, R. W., Hill, J. M., Coetzee, J. A., and Hill, M. P.: The contributions of biological control to reduced plant size and biomass of water hyacinth populations, Hydrobiologia, 807, 377–388, https://doi.org/10.1007/s10750-017-3413-y, 2018.

Kleinschroth, F., Winton, R. S., Calamita, E., Niggemann, F., Botter, M., Wehrli, B., and Ghazoul, J.: Living with floating vegetation invasions, Ambio, 50, 125–137, https://doi.org/10.1007/s13280-020-01360-6, 2021.

https://doi.org/10.5194/egusphere-2026-403
Preprint. Discussion started: 10 February 2026

Lin, Y., Li, L., Yu, J., Hu, Y., Zhang, T., Ye, Z., Syed, A., and Li, J.: An optimized machine learning approach to water pollution variation monitoring with time-series Landsat images, International Journal of Applied Earth Observation and Geoinformation, 102, 102370, https://doi.org/10.1016/j.jag.2021.102370, 2021.

Piaser, E. and Villa, P.: Evaluating capabilities of machine learning algorithms for aquatic vegetation classification in temperate wetlands using multi-temporal Sentinel-2 data, International Journal of Applied Earth Observation and Geoinformation, 117, 103202, https://doi.org/10.1016/j.jag.2023.103202, 2023.

Simpson, M. D., Akbari, V., Marino, A., Prabhu, G. N., Bhowmik, D., Rupavatharam, S., Datta, A., Kleczkowski, A., Sujeetha, J. A. R. P., Anantrao, G. G., Poduvattil, V. K., Kumar, S., Maharaj, S., and Hunter, P. D.: Detecting Water Hyacinth Infestation in Kuttanad, India, Using Dual-Pol Sentinel-1 SAR Imagery, Remote Sensing, 14, 2845, https://doi.org/10.3390/rs14122845, 2022.

Swinnen, E. and Toté, C.: Copernicus Global Land Operations “Vegetation and Energy” ”CGLOPS-1” ALGORITHM THEORETICAL BASIS DOCUMENT NORMALIZED DIFFERENCE VEGETATION INDEX (NDVI) COLLECTION 300M, 2022.

Thamaga, K. H. and Dube, T.: Testing two methods for mapping water hyacinth (Eichhornia crassipes) in the Greater Letaba river system, South Africa: discrimination and mapping potential of the polar-orbiting Sentinel-2 MSI and Landsat 8 OLI sensors, International Journal of Remote Sensing, 39, 8041–8059, https://doi.org/10.1080/01431161.2018.1479796, 2018.

Tilstra, L. G., de Graaf, M., Trees, V. J. H., Litvinov, P., Dubovik, O., and Stammes, P.: A directional surface reflectance climatology determined from TROPOMI observations, Atmospheric Measurement Techniques, 17, 2235–2256, https://doi.org/10.5194/amt-17-2235-2024, 2024.

Tucker, C. J.: Red and photographic infrared linear combinations for monitoring vegetation, Remote Sensing of Environment, 8, 127–150, https://doi.org/10.1016/0034-4257(79)90013-0, 1979.

Villa, P., Mousivand, A., and Bresciani, M.: Aquatic vegetation indices assessment through radiative transfer modeling and linear mixture simulation, International Journal of Applied Earth Observation and Geoinformation, 30, 113–127, https://doi.org/10.1016/j.jag.2014.01.017, 2014.

Wilson, J. R., Holst, N., and Rees, M.: Determinants and patterns of population growth in water hyacinth, Aquatic Botany, 81, 51–67, https://doi.org/10.1016/j.aquabot.2004.11.002, 2005.

Worqlul, A. W., Ayana, E. K., Dile, Y. T., Moges, M. A., Dersseh, M. G., Tegegne, G., and Kibret, S.: Spatiotemporal Dynamics and Environmental Controlling Factors of the Lake Tana Water Hyacinth in Ethiopia, Remote Sensing, 12, 2706, https://doi.org/10.3390/rs12172706, 2020.